ASGE Vol. 06 (01), pp. 87-100, 2022

Egyptian Knowledge Bank

International Journal of Advances in Structural and Geotechnical Engineering

https://asge.journals.ekb.eg/

Print ISSN 2785-9509 Online ISSN 2812-5142

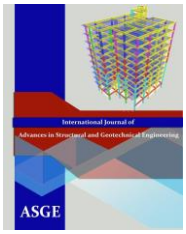

Experimental Investigation of Cyclic Performance of Slotted RC Beam-Column Connection

Mohamed A. Sakr [1], Ayman A. Seleemah[2], Tarek M. Khalifa[3], and Esam A. Darwish[4]

[1,2] Professor, Faculty of Engineering, Tanta University, Egypt

E-mail: mohamed.sakr2@f-eng.tanta.edu.eg - seleemah@f-eng.tanta.edu.eg

[3]Associated Professor, Faculty of Engineering, Tanta University, Egypt

E-mail: tarek.khalifa@f-eng.tanta.edu.eg

[4]Assistant lecturer, Faculty of Engineering, Tanta University, Egypt

E-mail: essam.darwish@f-eng.tanta.edu.eg

ABSTRACT

The slotted RC beam-column connection was introduced as a promising low-damage beam-column connection substitute for conventional design. It consists of a conventional RC beam, modified with a narrow vertical slot adjacent to the column face, running approximately three-quarters of the beam depth. In this study, quasi-static cyclic experimental tests were performed on in-plan conventional RC beam-column subassembly RCB and slotted RC beam-column subassembly SL to compare the response of slotted-beams with the conventional monolithic beam and verify the reduction in damage to the connection .

The experimental program has demonstrated that the reinforced concrete slotted beam-column subassembly is a viable substitution for the monolithic detail. Extremely promising structural performance was observed. High energy dissipation and stable response were observed to 3.5% beam drift. The system displayed reduced levels of damage to the plastic hinge zone when compared to conventional monolithic subassembly. Beam elongation for the slotted beam was shown to be significantly less than traditional reinforced concrete beams.

Keywords: Slotted RC beam column connection, Low cyclic fatigue, low damage, Experimental.

INTRODUCTION

Past earthquake observations and subsequent laboratory works proved that beam column connections have a key role in reinforced concrete (RC) structures, as it is responsible for maintaining the integrity of the whole structure, determining the ductile/nonductile, and strength degradation behavior of moment frames. Failure of such connections can result in a global structural collapse, Fig. 1. Inadequate shear resistance of beam-column joints is one of the most severe deficiencies in RC frame structures that make it vulnerable against earthquakes, Fig. 2 , [1-3].

ACI 352 report in particular ACI 352, 1985, implicitly accept a high level of damage in the form of shear cracking, bar slip and possible column flexural hinging for joints in moment frames subjected to large lateral load reversals. There have been several updates to the ACI 352 original document (ACI 352R, 2002) that have added additional qualifications, provisions, and commentary to the original version, but the basic design values have not changed significantly. The New Zealand approach, since the mid-1980s (NZS3101, 1982) has been to minimize that type of damage and concentrate the deformations in plastic hinges in the beams by careful detailing of the joint region and explicit capacity-design of the joint and columns [4].

(a) (b)

Fig. 1 (a) Collapsed building from the August 17, 1999 Kocaeli Earthquake [5] (b) Damage to 15-story building in the September 21, 1999 Chi-Chi Taiwan Eq.

Fig. 2 Severe damage in beam column connection in RC building, L'Aquila Earthquake, Italy -2009. [3]

According to Fenwick at al. [6], in reinforced concrete structures, plasticity is provided through the formation of plastic hinges. There are two types of plastic hinges that can form in moment resisting reinforced concrete frames: unidirectional and reversing. These plastic hinge types are shown in. The type of plastic hinge that forms is dependent on the building geometry, loading and detailing. Several unwanted consequences are associated with plastic hinge formation.

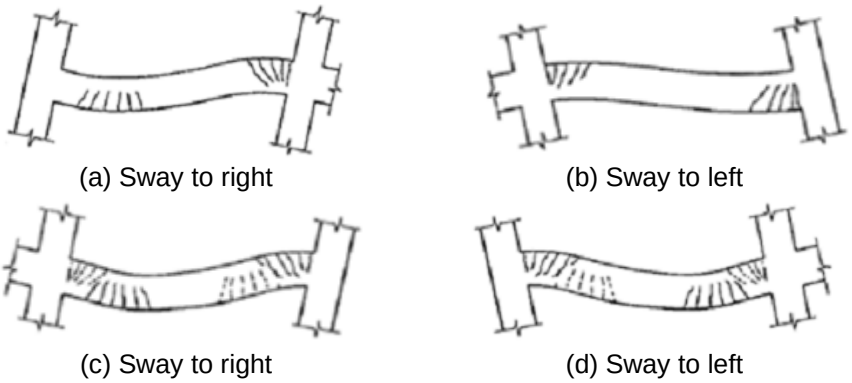

(a) Sway to right (b) Sway to left

(c) Sway to right (d) Sway to left

Fig. 3 Uni-directional (a & b) and reversing (c & d) plastic hinges [6]

The first consequence is damage to the structural elements. The cracking of concrete necessitated to provide adequate ductility means that at the end of a significant seismic event the plastic hinge zones are heavily damaged, such as shown in Fig. 4 . Following the 1995 Kobe and 2011 Christchurch earthquakes there were examples of buildings that had formed plastic hinges, as designed, being demolished due to prohibitive rehabilitation costs [6].

Fig. 4 Damage of ductile Beam Column Joint at the Price Waterhouse Coopers Building-New Zealand at 22 Feb 2011 Christchurch earthquake [6]

A further consequence of plastic hinge formation is beam elongation. It has been shown that over the course of a significant seismic event a plastic hinge can lengthen by 2-5% of the beam depth[6, 7]. Beam elongation can be attributed to two main contributors: geometric and material. The geometric contribution stems from the points of rotation at either beam end not being coincident for a traditional reinforced concrete beam. Hence, this contribution is more prevalent in deep beams and structures that are subject to large drift demands. A schematic of the geometric beam elongation mechanism is shown in Fig. 5.

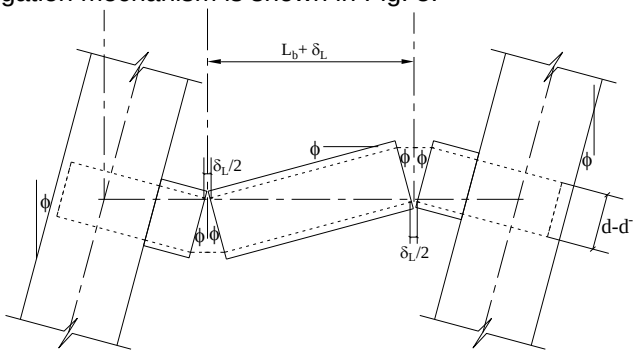

Fig. 5 schematic of the geometric beam elongation mechanism

In light of this, providing low-cost, high-seismic performance structures capable of sustaining a design level earthquake with limited or negligible damage, and minimum disruption of business, became an utmost necessity. The slotted-beam column connection system was first introduced in 1999 [8]. It was investigated as a promising non-tearing floor substitute for conventional design. It consists of a conventional reinforced concrete beam, modified with a narrow vertical slot adjacent to the column face, Fig. 6, running approximately three-quarters of the beam depth. Seismic rotations occur about the remaining concrete “top-hinge”, such that deformations are concentrated in the bottom bars of the beam, away from the floor slab, and beam elongation is minimized. The research carried out in this connection showed that, it is an effective low damage solution, which could provide a simple and practical substitute for conventional reinforced concrete beam column connection [9-13].

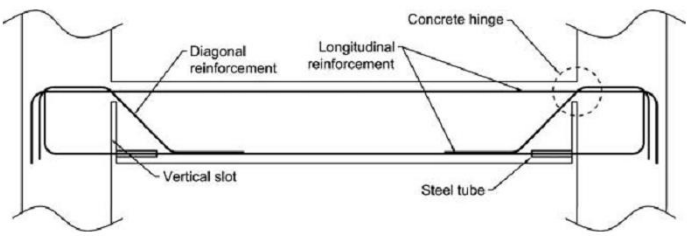

Fig. 6 Slotted RC beam-column connection

Development of Experimental Program

This test program was implemented at the structural laboratory of the Pacific Earthquake Engineering Research (PEER) Center of UC Berkeley under quasi-static cyclic loading. Development of the experimental program to investigate the structural behavior of exterior monolithic conventional RC beam column connection RCB as a reference specimen subjected to quasi-static cyclic loading compared to exterior slotted RC beam column connections with 120mm unbonded length SL subjected to the same loading protocol has been done. Design of the experimental specimens, construction, instrumentation, test setup, loading protocol, and material testing are also presented.

Conventional RC Beam Column connection (RCB)

This test specimen was designed according to ACI 352R-02 [14]. These recommendations are for determining proportions, design, and details of monolithic beam-column connections in cast-in-place concrete frame construction in seismic and non-seismic regions. The recommendations are written to satisfy strength and ductility requirements related to the function of the connection within a structural frame.

Fig. 7 shows the structural drawing for RCB. The column had a scaled inter storey height of 2.10 m and the beam had a cantilever span length of 1.60 m. The column has a side different longitudinal reinforcement with 3#4 on each side grade 60 bars with lower characteristic yield strength of 60000PSI (413MPa), and 2#4 grade 60 intermediate bars as shown at Fig. 3 1. The beam has equal top and bottom longitudinal reinforcement of 3#4 Grade 60 bars. The column and beam stirrups are #2.5 grade 40 with lower characteristic yield strength of 40000PSI (275.33Mpa) with different spacing according to the requirements of ACI 352R-02 as shown at Fig. 7. The concrete had a specified 28-day compressive strength $f_c^{\backslash}$ of 4000 PSI (27.57MPa).

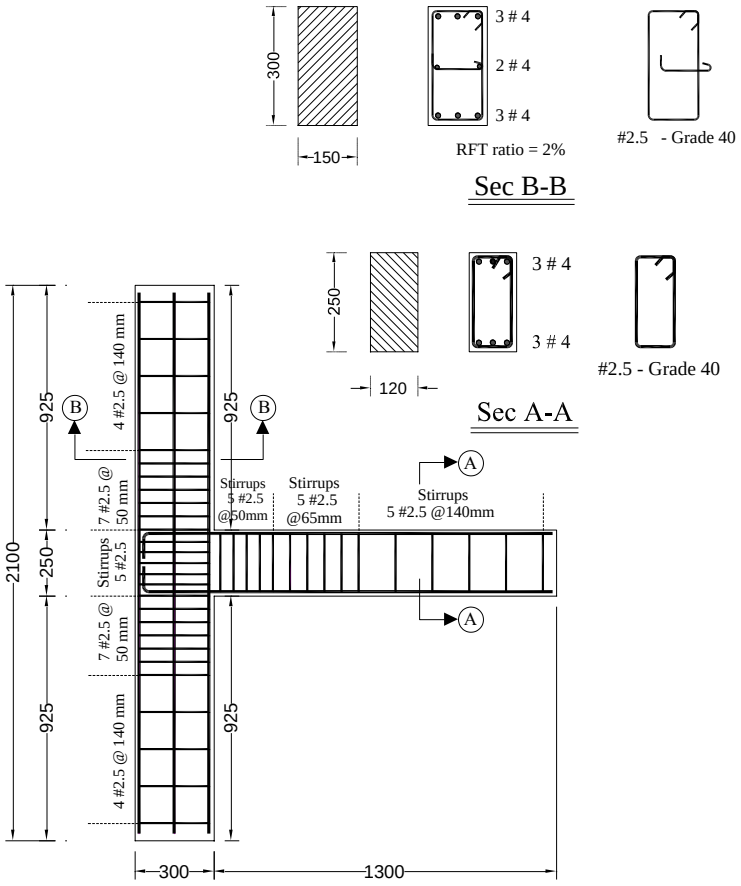

Fig. 7 Details of conventional Beam-Column connection RCB

Slotted RC beam column connection

Fig. 8 shows the structural drawing of the slotted RC beam column connection with 120mm unbonded length for the bottom rebars starting from the slot, which had identical geometry to benchmark specimen RCB. The slot adjacent to the column face was 12.00 mm width and running 187.5mm depth which is three quarters the depth of the beam. The slot width was sized to accommodate 4.5% drifts without contact between the beam soffit and column face.

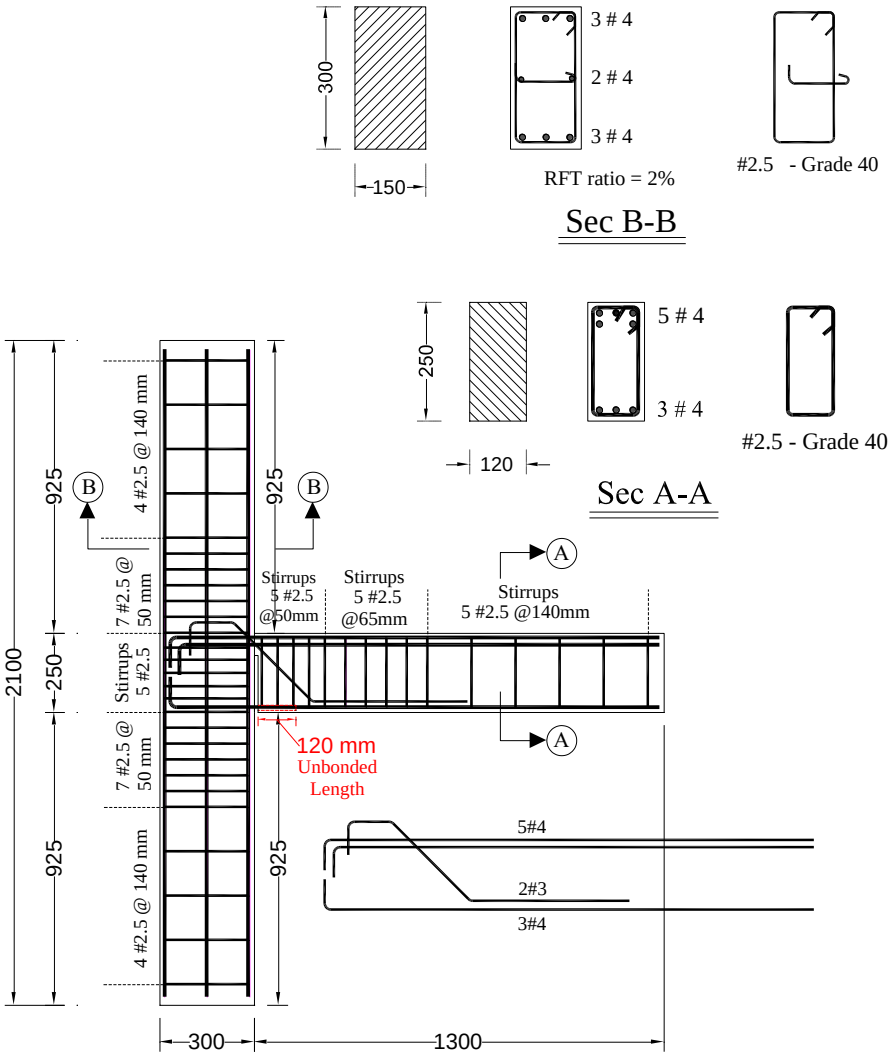

Fig. 8 Details of Slotted Beam-Column connection with 120mm unbonded length SL-120

The flexural capacity of the slotted RC beam column connection in positive (opening) and negative (closing) moments are governed by yielding of the bottom RFT, only this reinforcement needs to be sized for the flexural demand. To get the same nominal moment capacity of RCB in opening and closing moments, 3#4 grade 60 bars were used for the bottom reinforcement as shown at Fig. 8. To limit cracking and elongation through the concrete top-hinge, the top to bottom reinforcement ratio ($A_{ś}f_{ý}/A_{s}f_{y}$) was chosen to be 1.67, so 5#4 grade 60 bars were used for top reinforcement as shown in Fig. 8, where $A_{ś}$, $f_{ý}$, A_{s}, and f_{y} are the area and the yield strength of the top and bottom reinforcement respectively.

Diagonal reinforcement was used to carry beam shear force in to the joint [8, 10]. This method is simple, efficient, and can be easily designed and hence was adopted in this research. 2#3 grade 60 diagonal hangers were used with 45º angle. To ensure the survival of the connection during the test, extra restraint was provided in the region along the unbonded length of bottom

bars to prevent buckling of these bars. 5#2.5 grade 40 at 50mm stirrups were used, then 5#2.5 grade 40 at 65mm spacing were used Fig. 8.

Material Testing

Extensive material testing was conducted for concrete and reinforcing steel as part of the research program and is described here. Normal weight dry mixed concrete bags with 4000psi (27.57MPa) compressive strength were provided from a local commercial vendor. A minimum slump of 80mm was enough to ensure proper workability and flowability of the concrete into the joint area. Compressive strength tests were conducted under force control to monitor the strength of the concrete at the age of 28 days. Standard 6in×12in cylinders were used. Also, splitting tensile strength represents a lower bound of the tensile strength of concrete. The test was conducted using standard 6 in.×12 in. concrete cylinders according to ASTM C496-04 [ASTM 2004a]. The modulus of rupture test, or three-point flexural test, was performed using 3 in.×3 in.×12 in. concrete beams according to ASTM C293-07 [ASTM 2007]. Test results are presented in Table. 1. Reinforcement rebars testing was carried out using the hydraulic universal testing machine. Two different samples of deformed bars were tested, #3 (3/8 In.) and #4 (1/2 In.) grade 60 reinforcing bars. The results are presented in Table. 2 below with typical stress-strain profiles for each bar number shown in **Error! Reference source not found.**. Note that the yield stress was defined as the initial point where the slope of the elastic curve decreased, thus the low yield strengths for some of the bars.

Table. 1 Mechanical properties of the concrete

Specimen	Compressive Test			Splitting tension f_{ct}		Modulus of rupture f_r	
	Average cylinder Test Load kips	Average cylinder Compressive strength PSI (MPa)	St. dev.	Average ksi (MPa)	St. dev.	Average ksi (MPa)	St. dev.
RCB	104.33	3692 (25.50)	6028	344.67 (2.37)	6.25 (0.047)	1158.33 (7.98)	101 (0.69)
SL	102.50	3627 (25.00)	1601	-	-	-	-

Table. 2 Mechanical properties for deformed reinforcing steel

Sample	#3 Bar	#4 Bar
Yield Stress (MPa)	448	410
Yield Strain	0.0021	0.0021
Elastic Modulus (MPa)	213333	195238
Strain @ Onset of Work Hardening	0.0023	0.0023
Ultimate Stress (MPa)	601	652
Ultimate Strain	0.0081	0.009
Overstrength Factor	1.34	1.59

Loading Protocol

Cyclic quasi-static loading was used to simulate seismic action on beam column connections. A displacement-controlled loading system was used which applied increasing displacement until a specified displacement ratio was reached. The drift sequence in Fig. 9 was applied at the beam tip in accordance with American Concrete Institute (ACI) acceptance criteria for moment frames (ACI Committee 374, 2005). Test specimens were subject to 3 cycles at displacement ratio levels of 0.16%, 0.24%, 0.32%, 0.48%, 0.71%, 0.95%, 1.42%, 1.76%, 2.22%, 2.80%, 3.50%, 4.20%, and 4.94%. Smaller cycles, varying from 0.67 to 0.33 of the previous displacement, followed each large displacement set to close gaps between aggregates in the concrete. According to ACI 374.1-05, there is no obligation for an axial load to be applied to the column simultaneously with the application of the lateral displacement. However, a constant axial load

of 1340 lb (60 KN) was applied to the column, using hydraulic jack, this load was to prevent any movement of the specimen during the test, Fig. 9.

Test Setup

The specimen was tested at the structural laboratory of the Pacific Earthquake Engineering Research (PEER) Center of UC Berkeley under quasi-static cyclic loading. Strain measurements, including Digital Image Correlation (DIC) [15-18], strain gauges and LVDTs were used to measure the performance of the reinforcing steel bars and the concrete. The specimens were attached to the loading frame in horizontal position of the column and subjected to a horizontal lateral loading at the beam tip, Fig. 9. Four ¾ inch threaded post tension rods were used to attach the specimen against the loading frame to prevent any overturning during the test. To support the specimen against any horizontal movement during the test, a steel subassembly composed of two 20 in. × 20in. ×1.5in. steel plates connected to each other with three ¾ threaded post tensioned rods and one 2in. steel strut welded to10in. × 10in. ×1.0in box section bolted to the loading frame, Fig. 10.

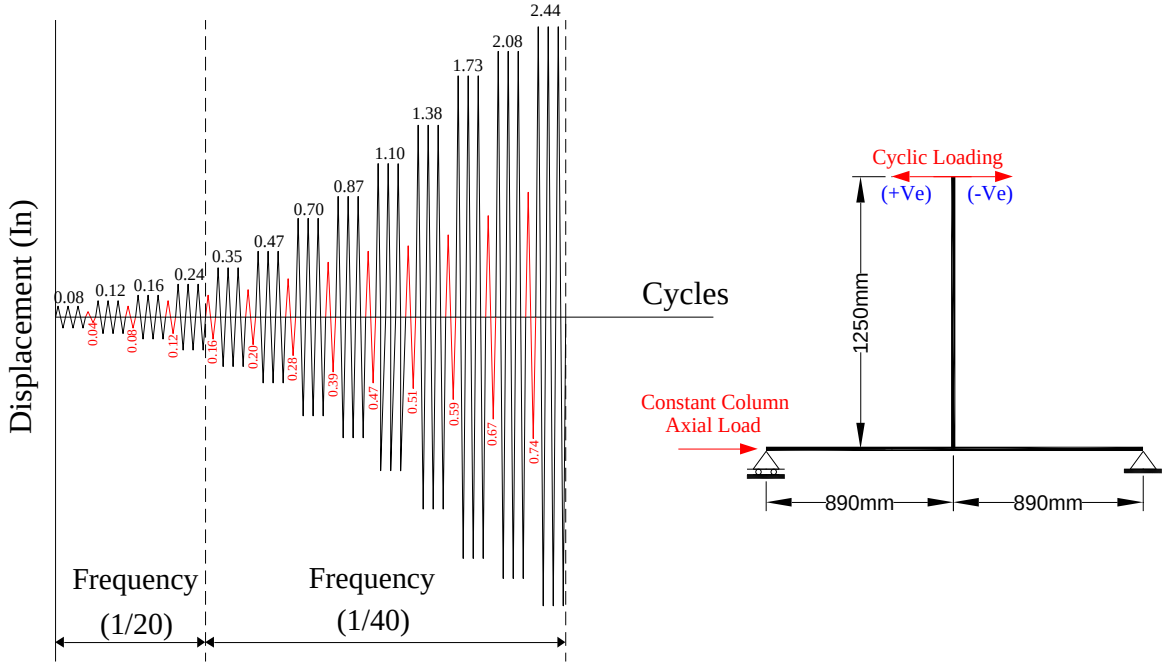

Fig. 9 Quasi Static Loading Protocol

To apply the constant column axial load of 60KN, a hydraulic jack connected to manual hydraulic oil pump , Fig. 10 and Fig. 11, was placed between one of the steel plates and the column upper end and pumped until reached the target load level and was maintained during the test. Displacement of the beam tip was measured using a wire potentiometer attached to the left column of the loading frame and connected to beam tip, Fig. 10 and Fig. 11. In case of any undesirable movement of the sample during the test, an LVDT was attached to the frontside face of the specimen. Drifts and relative deformations between the beam and the columns were measured using two different techniques, traditional technique using LVDTs at the backside of the specimen, Fig. 11 (b), and new technique with Digital Image Correlation DIC at the frontside face side.

On the frontside face of the specimen, digital image correlation 'DIC' was used to calculate complete surface displacement and strain fields of the specimens under test loading. The region of interest 'ROI' was first identified and a random speckle pattern with high contrast (black speckles over white paint) was applied to the specimen. as shown in Fig. 12a. Using Canon EOS 6D digital camera with Canon zoom lens EF 24-105mm 1:4 L IS USM and the focal lens

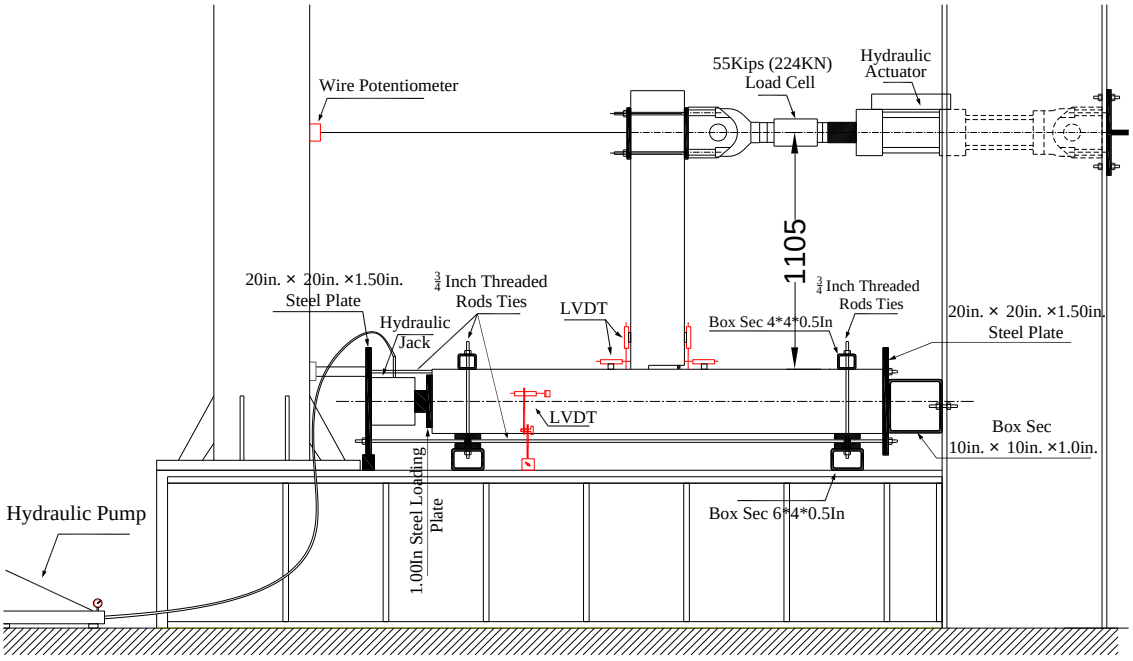

Fig. 10 Test Setup (Frontside Face)

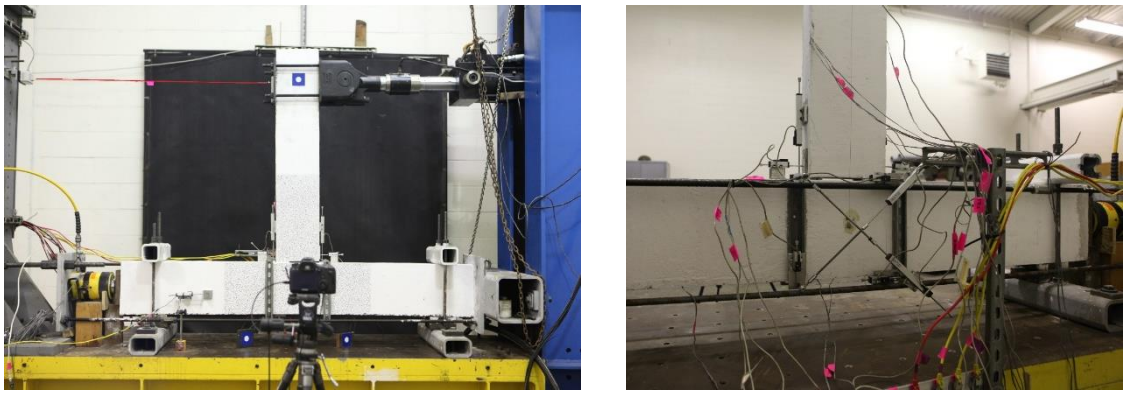

(a)Frontside face of the specimen *(b)Backside face of the specimen*

Fig. 11 Test Setup Photos

was adjusted to 50mm, 312 high resolution digital images were taken during the evolution of the test loading. The quality settings of the camera were adjusted to get RAW images with heights quality, Fig. 12b. Camera Setup for the test is shown in Fig. 11. The software package **Optecal** was used to process the images for the DIC. For more details on the DIC technique.

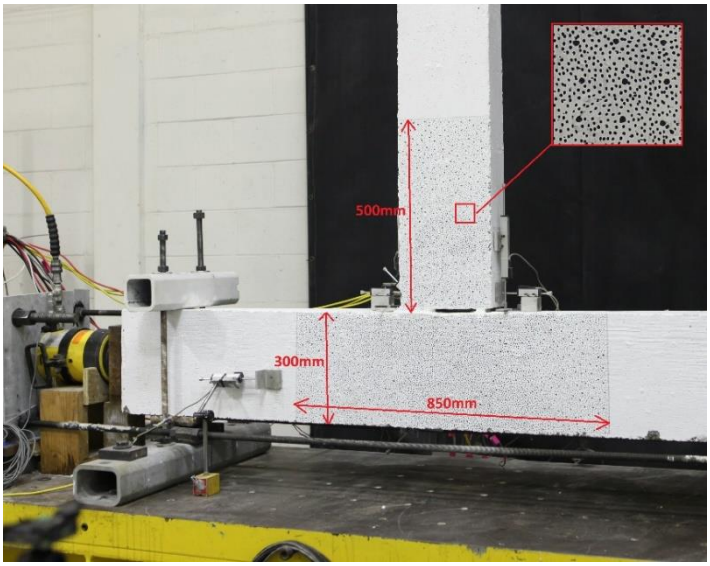

(a)Region of interest (ROI) and applied speckle pattern on the specimen frontside face

(b)Camera used for DIC

Fig. 12 Region of interest (ROI), applied speckle pattern, and camera settings for DIC

Test Results

The results obtained from the experimental test are presented here. Behavior of conventional RC beam column connection is compared to behavior of slotted beam column connections.

General behaviour and hysteresis response

Applied force versus drift ratio response for the conventional beam column connection RCB and slotted connection SL are shown in Fig. 13. Fig. 14 shows the drift ration versus beam shear sliding of the different test modules. As shown in Fig. 13, a stable, typical reinforced concrete hysteresis up to 5.6% drift ratio. Pinching of the hysteresis curve because of beam shear sliding was first observed at 1.71% drift ratio (0.85in) at 37 KN applied force as shown in Fig. 13 and Fig. 14. A much fatter steel-like hysteresis curve for the slotted connection SL compared to the conventional connection RCB. This can be explained by the very small value of beam shear sliding compared to the conventional connection as shown in Fig. 14.

For RCB, first flexure crack occurred at 0.48% drift ratio (0.24 in) at 17.33 KN applied force in the positive direction (opening moment) as shown at Fig. 15 a, while it was occurred at -19.76 KN applied force in the negative direction (closing moment) as shown at Fig. 15 b, and followed by penetration crack inside the column around the beam top longitudinal reinforcement at the same applied load and drift ratio, Fig. 15 b. For the slotted connection, SL, compared to RCB, first flexure cracks in opening and closing directions occurred at higher drift ratios at +0.71% drift ratio (+0.35 in) at +24 KN applied force (opening moment) and -26.61 KN applied force in the negative direction (closing moment) respectively, about twice the corresponding value of

drift ration of RCB, accompanied by longitudinal top and bottom reinforcement penetration crack at the column, Fig. 15. For RCB, Joint diagonal crack was first observed in closing direction then in opening direction at the same drift ratio as SL connection at 0.71% drift ratio (0.35 in) at 36.6 KN applied force.

Yielding of beam bottom longitudinal reinforcement in tension for RCB was observed at 1.10% drift ratio (0.56 in), at an applied force of 35.4 KN, Fig. 13 a, while yielding of beam top longitudinal reinforcement was observed at -1.20% drift ratio (-0.616 in), at an applied force of -35.58 KN in closing direction, Fig. 13. For SL connection, yielding of bottom longitudinal reinforcement in tension was observed at 1.10% drift ratio (0.56 in), at an applied force of 33 KN which is a little lower than RCB, while yielding of top longitudinal reinforcement was observed at -3.10% drift ratio (-1.53 in), at an applied force of -42.2 KN in closing direction.

Unlike RCB, bottom reinforcement parallel crack was observed at the beam soffit due to buckling of beam bottom longitudinal reinforcement at cycle number 21 at +0.95% drift ratio (0.47in) corresponding to +30 KN, Fig. 16.

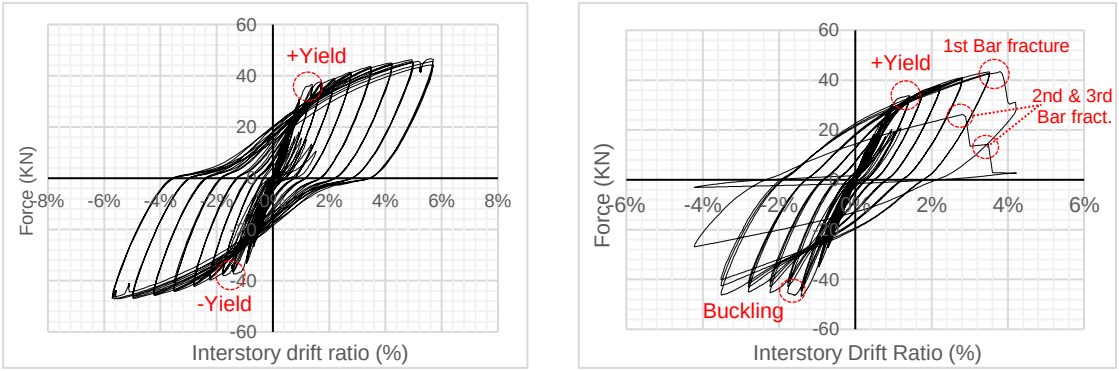

(a) RCB connection (b) SL connection

Fig. 13 Hysteresis curves of test specimens

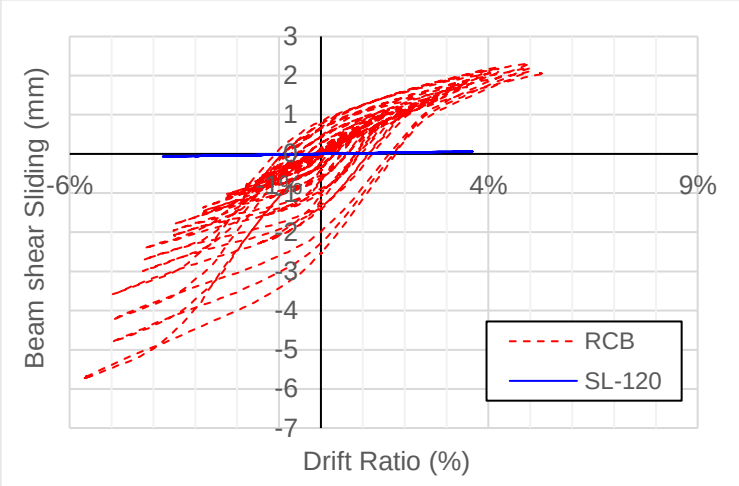

Fig. 14 Drift ratio - Beam shear sliding relationship.

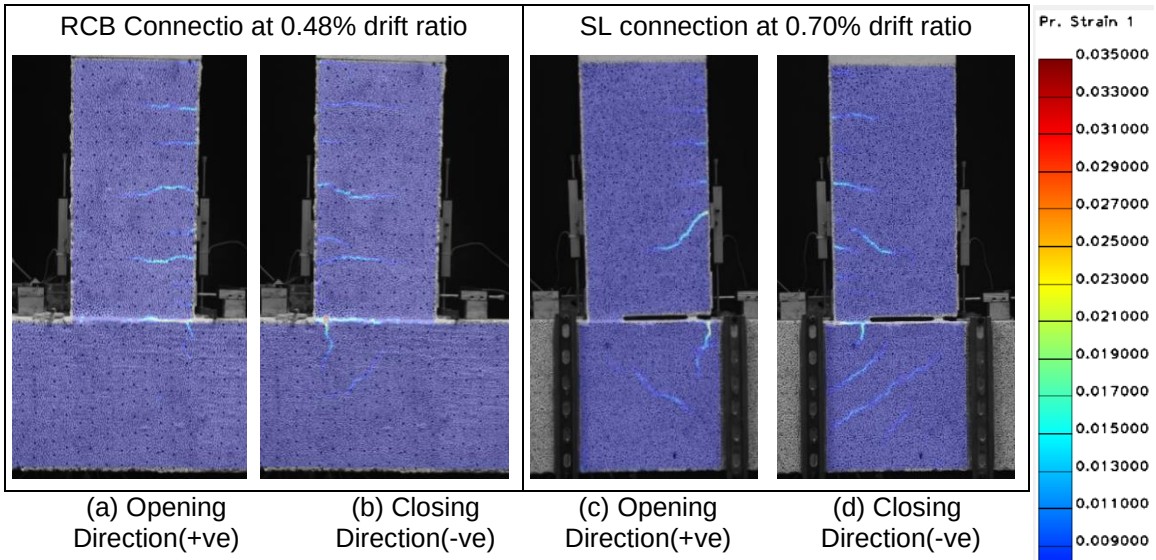

Fig. 15 First flexural Crack (DIC-Principal tensile strain)

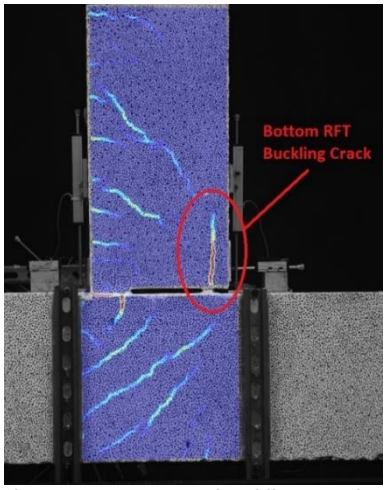

Fig. 16 Bottom RFT buckling crack of specimen SL at 0.95% drift ratio.

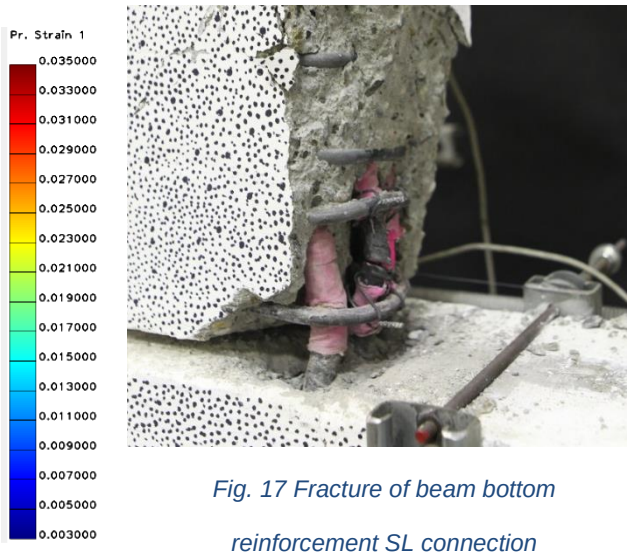

Fig. 17 Fracture of beam bottom reinforcement SL connection

Fracture of beam bottom reinforcement due to low cyclic fatigue was first occurred at cycle number 45 at +3.80% drift ratio (+1.87in) at +43.36KN for one of the three beam bottom rebars resulting in a sudden loss of the beam flexural resistance loss by 13.11 KN which is about 30% of the beam resistance at this stage, Fig. 13 b. In the next opening cycle, cycle number 46, at the same time, fracture of the remaining two rebars was occurred resulting in a total loss of the beam flexural resistance, Fig. 13 b and Fig. 17. Because the behaviour of the slotted connections in opening and closing moment is governed by yielding of the lower beam reinforcement, like the conventional connections, the ultimate load capacity of SL-120 at the maximum reached drift ratio in opening direction is almost the same of RCB, Fig. 13.

Crack Development and Observed Damage

Fig. 18 a through d shows the observed damage at 3.5% drift ratio as maximum principal tensile strain using DIC for both test modules. In general, the overall performance of SL was extremely satisfactory. A stable response was observed to 3.5% beam drift with high levels of hysteretic energy dissipation observed.

Specimen SL exhibited very little damage and cracking compared to RCB. In the opening and closing moments, Fig. 18 a throught c, the maximum crack width within the beam-column subassembly RCB is about 2.5 times that for SL. It also illustrates the development of cracks on the face of the specimen. For SL specimen, all flexural cracks along the beam and column lengths where reinforcement remained elastic and closed on unloading. Significant flexural cracking was concentrated into the concrete top-hinge and around the unbonded length of beam bottom reinforcement as shown in Fig. 18.

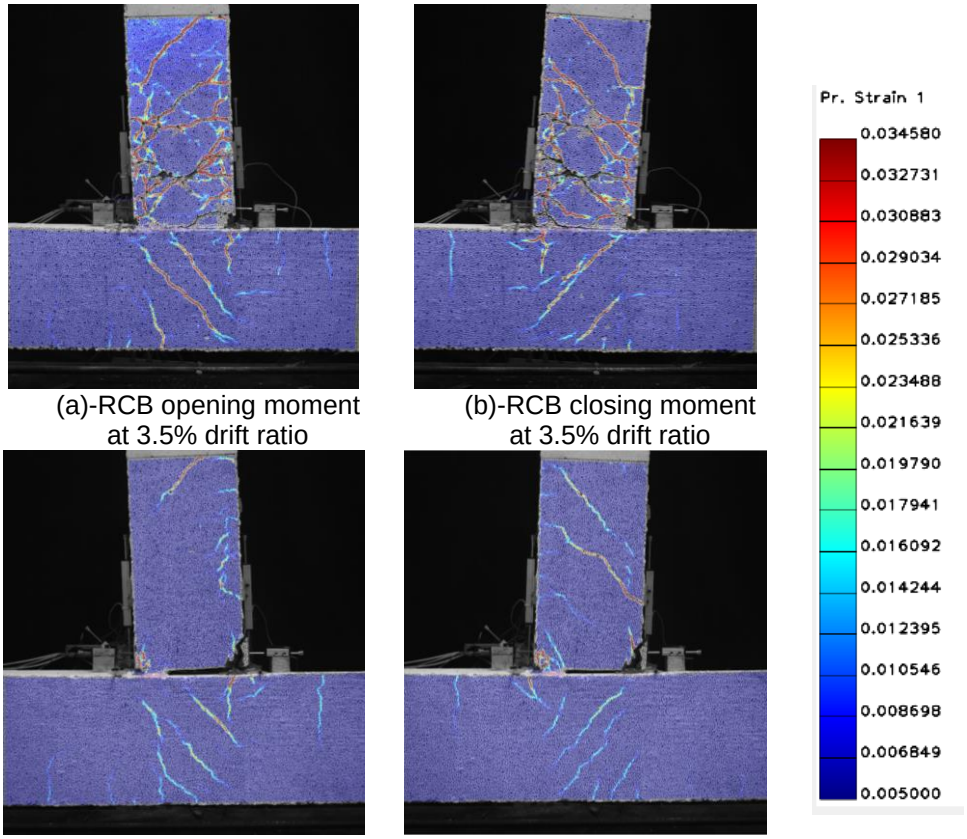

(a)-RCB opening moment at 3.5% drift ratio

(b)-RCB closing moment at 3.5% drift ratio

(c)-SL opening moment at 3.5% drift ratio

(d)-SL closing moment at 3.5% drift ratio

Fig. 18 Observed damage at 3.5% drift ratio for different test modules

(DIC-Principal tensile strain)

CONCLUSION

Experimental investigation for the behavior of conventional reinforced concrete beam-column subassembly compared to reinforced concrete slotted beam-column connection has been conducted. The experimental testing has been summarised and the selected results presented and discussed.

The experimental program has demonstrated that the reinforced concrete slotted beam-column subassembly is a viable substitution for the monolithic detail. Extremely promising structural performance was observed. High energy dissipation and stable response were observed to 3.5% beam drift. The system displayed reduced levels of damage to platic hinge zone when compared to convetional monolithic subassembly. Beam elongation for the slotted beam was shown to be significantly less than traditional reinforced concrete beams.

On the other hand, because the plastic strain accumulation in bottom longitudinal reinforcement, slotted-beams are more at risk to low cycle fatigue failure. This is clearly shown

in the premature mode of failure of the beam lower rebars. Which requires intensive investigation to avoid such mode of failure.

ACKNOWLEDGEMENTS

This research was made possible by support provided by Prof. Khalid Mosalam Director of Pacific Earthquake Engineering Resrech Center PEER, University of California, Berkeley. Thanks are extended to PEER Associate Director Amarnath Kasalanati and Arpit Nema Postdoctoral Researcher, Richmond Field Station.

REFERENCES

1. El-Amoury, T. and A. Ghobarah, *Seismic rehabilitation of beam–column joint using GFRP sheets.* Engineering Structures, 2002. **24**(11): p. 1397-1407.
2. Tasligedik, A.S., et al., *Strength Hierarchy at Reinforced Concrete Beam-Column Joints and Global Capacity.* Journal of Earthquake Engineering, 2018. **22**(3): p. 454-487.
3. Mosalam, K.M. and M.S. Günay, *Structural Engineering Reconnaissance of the April 6, 2009, Abruzzo, Italy, Earthquake, and Lessons Learned* in *PEER Report 2010/105*. April 2010, College of Engineering, University of California, Berkeley: Pacific Earthquake Engineering Research Center
4. Roberto T. Leon, W.Y.K. and P. Stefano, *Performance of Beam-Column Joints in the 2010-2012 Christchurch Earthquakes.* ACI Symposium Publication. **296**.
5. Saatcioglu, M., et al., *The August 17, 1999, Kocaeli (Turkey) earthquake damage to structures.* Canadian Journal of Civil Engineering, 2001. **28**: p. 715-737.
6. Fenwick, R.C. and L.M. Megget, *Elongation and load deflection characteristics of reinforced concrete members containing plastics hinges.* Bulletin of the New Zealand National Society for Earthquake Engineering, 1993. **26**(1): p. 28-41.
7. Liddell, D., J.M. Ingham, and B.J. Davidson, *Influence of loading history on ultimate displacement of concrete structures*. 2000: Department of Civil and Resource Engineering, University of Auckland.
8. Ohkubo, M., et al., *Shear Transfer Mechanism of Reinforced Concrete Beams with a Slot at the Beam-end.* 1999. **21**(3): p. 523-528.
9. OHKUBO, M. and T. HAMAMOTO, *Developing reinforced concrete slotted beam structures to reduce earthquake damage and to enhance seismic structural performance*, in *13th World Conference on Earthquake Engineering*. 2004: Vancouver, B.C., Canada
10. Au, E.V., *The mechanics and design of a non-tearing floor connection using slotted reinforced concrete beams* in *Department of Civil and Natural Resources Engineering* 2010, University of Canterbury, Christchurch, New Zealand: University of Canterbury, . p. 349.
11. Muir, C.A., S. Pampanin, and D.K. Bull, *Experimental method and results from seismic testing of a two-storey, two-by-one bay, reinforced concrete slotted beam superassembly*, in *15 WCEE LISBOA 2012*. 2012.
12. Muir, C.A., S. Pampanin, and D.K. Bull, *Background, design and construction of a two-storey, two-by-one bay, reinforced concrete slotted beam superassembly* in *15 WCEE LISBOA 2012*. 2012.
13. Muir, C.A., D.K. Bull, and S. Pampanin, *Preliminary observations from biaxial testing of a two-storey, two-by-one bay, reinforced concrete slotted beam superassembly* BULLETIN OF THE NEW ZEALAND SOCIETY FOR EARTHQUAKE ENGINEERING, September 2012. **Vol. 45**: p. 97-104.
14. American concrete institute, *Recommendations for Design of Beam-Column Connections in Monolithic Reinforced Concrete Structures*, in *ACI 352R-02*. 2002, ACI-ASCE Committee 352.
15. McCormick, N. and J. Lord, *Digital image correlation for structural measurements.* 2012. **165**(4): p. 185-190.
16. Reagan, D., A. Sabato, and C. Niezrecki, *Feasibility of using digital image correlation for unmanned aerial vehicle structural health monitoring of bridges.* Structural Health Monitoring, 2017. **17**(5): p. 1056-1072.

17. Tekieli, M., et al., *Application of Digital Image Correlation to composite reinforcements testing.* Composite Structures, 2017. **160**: p. 670-688.
18. Hassan, G.M., *Deformation measurement in the presence of discontinuities with digital image correlation: A review.* Optics and Lasers in Engineering, 2021. **137**: p. 106394.